Venusian channel formation as a subsurface process

Nicholas P. Lang[1] and Vicki L. Hansen[1]

Received 29 October 2005; revised 18 December 2005; accepted 19 January 2006; published 1 April 2006.

[1] We constructed detailed geologic maps of channels within three widely separated regions using Magellan synthetic aperture radar (SAR) imagery and altimetry radar data in order to understand the operative processes involved in Venusian channel formation. Channels in each region cut topographic highs including ridges and shield edifices with no deflection of the channel course by surface topography. We argue that these relationships are difficult to reconcile with the widely held view that Venusian channels represent surface processes, whether constructional or erosional. We conclude that the channels evolved through subsurface fluid flow, which involved local stoping and transport of overlying material; that is, these channels were carved from below, rather than from above. We postulate that at least some Venusian channels form because of subsurface fluid flow along a shallow crustal interface that forms the boundary between overlying low backscatter surface materials and underlying basal materials. Fluid movement along the interface may facilitate piecemeal stoping and erosion of the local surface materials from below, eventually resulting in the formation of channel traces exposed at the surface. The low backscatter material which hosts the channels in this study also hosts abundant coalescing shields and associated deposits, which may represent shield terrain.

Citation: Lang, N. P., and V. L. Hansen (2006), Venusian channel formation as a subsurface process, *J. Geophys. Res.*, *111*, E04001, doi:10.1029/2005JE002629.

1. Introduction

[2] Channels are a common feature across the surface of Venus [*Baker et al.*, 1992; *Komatsu et al.*, 1993], and understanding their formation represents a challenging puzzle in Venus's geologic record. Venusian channels, open conduits believed to have transported fluid [*Baker et al.*, 1992], are morphologically classified as simple, complex, and compound [*Gulick et al.*, 1991; *Baker et al.*, 1992]; a single channel may display all three morphologic classifications [*Baker et al.*, 1997]. Despite morphologic differences, Venusian channels share some similar characteristics with terrestrial channels. For example, the sinuosity and meander properties of Venusian channels resemble terrestrial fluvial systems [*Komatsu and Baker*, 1994]. However, unlike terrestrial fluvial systems, many Venusian channels typically maintain constant widths of $<1-3$ km along lengths up to >1000 km [*Baker et al.*, 1992] and lack tributaries, cutoff meanders, and extensive lateral flow deposits. In addition, Venusian channels are abundant in presumed volcanic regions [*Komatsu et al.*, 1993] where sources and termini are generally indistinct [*Baker et al.*, 1997] and channels maintain low gradients [*Baker et al.*, 1992], reach depths up to tens of meters [*Komatsu et al.*, 1992, 1993], and locally display what appear to be levees [*Komatsu et al.*, 1992; *Bussey et al.*, 1995]. Collectively, these characteristics make Venusian channels intriguing features on Venus's surface.

[3] Workers agree about channel characteristics, and they generally agree that fluids played a major role in sculpting channels [*Baker et al.*, 1992; *Komatsu et al.*, 1992, 1993; *Komatsu and Baker*, 1994; *Gregg and Greeley*, 1993; *Kargel et al.*, 1994; *Bussey et al.*, 1995; *Williams-Jones et al.*, 1998; *Jones and Pickering*, 2003]. Channel association with presumed volcanic regions [*Komatsu et al.*, 1993] and current surface conditions on Venus ($\sim$450°C [*Crisp and Titov*, 1997], $\sim$100 bars [*Fegley et al.*, 1997]) has led many workers, including us, to infer a volcanic origin for channels, although origins involving liquid water cannot be fully excluded [*Baker et al.*, 1992; *Jones and Pickering*, 2003; *Donahue et al.*, 1982, 1997]. In order to accommodate Venusian channel characteristics and surface conditions, a diversity of fluids and channel forming mechanisms have been proposed. However, all hypotheses of channel formation include the assumption that channels form at the atmosphere-surface interface. Hypotheses also include the assumption that channels form in a substrate of basalt [*Baker et al.*, 1992; *Komatsu et al.*, 1992, 1993; *Komatsu and Baker*, 1994; *Gregg and Greeley*, 1993; *Kargel et al.*, 1994; *Bussey et al.*, 1995; *Williams-Jones et al.*, 1998], although *Jones and Pickering* [2003] proposed a sediment substrate carved by water. Therefore, similar to Earth, the role of the chemical and physical properties of the surface environment, fluid, and substrate must each be considered when addressing processes of Venusian channel formation. On Earth, lava channels form from constructional processes as well as from mechanical, thermal, and thermomechanical erosion and it seems plausible to consider that the same

[1]Department of Geological Sciences, University of Minnesota Duluth, Duluth, Minnesota, USA.

0148-0227/06/2005JE002629$09.00

processes of channel formation operate on Venus. Constructional processes involve the formation of levees to constrain fluid flow [*Hulme*, 1974]; levees will begin to form as lava cools. Mechanical erosion occurs by fluid physically plucking material from the substrate and is enhanced by turbulent fluid flow [e.g., *Kargel et al.*, 1994; *Williams-Jones et al.*, 1998]. Thermal erosion results from melting of the substrate [*Hulme*, 1973, 1982; *Carr*, 1974; *Dawson*, 1990; *Komatsu et al.*, 1992; *Bussey et al.*, 1995; *Greeley et al.*, 1998; *Fagents and Greeley*, 2001; *Kerr*, 2001; *Williams et al.*, 2004]. Thermomechanical erosion involves aspects of both mechanical and thermal erosion [*Fagents and Greeley*, 2001]. The efficiency of the proposed erosional channel-forming processes will depend largely on lava cooling rate, although physical properties of the lava and substrate also play a role [e.g., *Williams et al.*, 1998; *Kerr*, 2001]. Consider, for example, a basalt flowing on a basaltic substrate. If the basalt flows in a turbulent regime, it will lose heat in an efficient manner [*Sakimoto and Zuber*, 1998] and not mechanically carve an extensive channel [*Komatsu et al.*, 1992]. However, lava such as alkali-carbonatite or sulfur may possibly flow turbulently, and mechanically carve channels on a basaltic substrate, for distances up to thousands of kilometers [*Kargel et al.*, 1994; *Williams-Jones et al.*, 1998]. Furthermore, both thermal and thermomechanical erosion require sufficient time to supply enough energy to the substrate to induce melting. Hence the rate of lava heat loss will govern the amount of thermal and thermomechanical erosion that occurs [*Hulme*, 1973; *Greeley et al.*, 1998; *Fagents and Greeley*, 2001; *Kerr*, 2001; *Keszthelyi*, 1995; *Sakimoto and Zuber*, 1998]. Thermal erosion will be more pronounced the greater the difference between the melting temperature of the substrate and the eruption temperature of the lava [*Greeley et al.*, 1998; *Williams et al.*, 1998; *Fagents and Greeley*, 2001]. For example, *Fagents and Greeley* [2001] demonstrated that basalt can thermomechanically erode a basaltic substrate. However, erosion remained concentrated near the vent because the basalt lava cooled too quickly to sustain erosion of basalt substrate. Conversely, *Williams et al.* [1998] demonstrated that komatiite lava can thermomechanically erode sediment substrate to create channels up to tens of kilometers long. Hence the cooling rate of lava on Earth contributes to the extent to which mechanical, thermal, and thermomechanical erosion may occur. Earth's atmosphere facilitates radiative cooling of lava flows [*Snyder*, 2002], which impedes the degree to which lava induced erosion occurs on Earth [e.g., *Fagents et al.*, 2001]. Conversely, Venus's CO_2-rich atmosphere acts as an insulating cover that impedes the loss of thermal energy from the surface, which allows lava flows to travel further on Venus than on Earth [*Snyder*, 2002]. The impeded cooling rate should enhance erosional processes compared to Earth. Clearly, many questions regarding the formation of Venusian channels still exist.

[4] The purpose of this contribution is to revisit questions of Venusian channel genesis. Similar to *Baker et al.* [1992], we broadly define channel as any open passage that likely transported fluid; however, we define conduit as a covered passage similar to a pipe. Because a single channel may display characteristics of all three morphologic classifications [*Baker et al.*, 1997], we avoid the channel classification schemes of *Gulick et al.* [1991] and *Baker et al.* [1992] in addressing channel formation. We focus our study by addressing the fundamental question: What are the operative processes of channel formation on Venus? We use full-resolution Magellan imagery and altimetry data in order to construct detailed geologic maps with the express goal of delineating the geologic history of specific channels. We select three widely separated study areas for the analysis. We conclude that the geologic relations for the channels highlighted here are consistent with their formation by subsurface stoping and erosion. We outline a hypothesis explaining channel formation as a subsurface process assuming some variety of lava carved the channels under current climatic conditions. Further, we discuss a possible candidate for the eroded material and implications for the channel forming lava.

2. Study

[5] To address questions of Venusian channels, we constructed geologic maps of channels and their surroundings in three widely separated study areas (Figure 1). Area one, the Kahlo Crater region (KCR; centered at 58°S, 173°E), is located in southern Nsomeka Planitia and hosts parts of three distinct channel traces named Citlalpul, Nahid, and Vesper Valles. Area two, the Norna Tessera region (NTR; centered at 49°S, 268°E), is located in southeast Helen Planitia and hosts a series of disconnected channel traces collectively named Sinann Vallis. Area three, the Atropos Tessera region (ATR; centered at 68.5°N, 308°E), is located in western Ishtar Terra and hosts Lunang Vallis.

[6] The field sites are located in two topographic provinces. Lowlands (expanses of gentle, long wavelength ($\sim$1000 km) basins) comprise the KCR and NTR field sites. The ATR field site is located in western Ishtar Terra (an anomalous highland region in Venus's northern hemisphere [*Kaula et al.*, 1997]). Channels in all three study areas occur within low backscatter material that is composed of numerous shield edifices, or shields and associated deposits. Shields, typically interpreted as volcanic constructs, are circular to quasi-circular features that are cone, flat-topped, dome, or shield shaped, generally $\ll$1 km in height, and typically <1–2 km in diameter [*Aubele and Slyuta*, 1990; *Head et al.*, 1992; *Guest et al.*, 1992; *Crumpler et al.*, 1997; *Addington*, 2001]. Shield size is difficult to constrain because shield bases are typically poorly defined and appear to blend into surrounding material that likely represents material erupted from the shield edifices [e.g., *Guest et al.*, 1992; *Hansen*, 2005]. Individual shield deposits appear to remain local to the shield, although quantifying the extent of an individual flow is difficult as deposits from surrounding shields typically coalesce. Locally, shields do not appear directly associated with any larger-scale volcanic and/or tectonic feature and do not appear to define a discernable pattern with regard to one another or other geologic features. We map the low backscatter material in each study area as a composite unit of flow material and edifices named unit lbm. As unit lbm is a composite unit, it cannot be used for more than local stratigraphic correlations [e.g., *DeShon et al.*, 2000; *Young and Hansen*, 2003]. In addition, KCR and NTR have secondary structures including fractures and wrinkle ridges. Wrinkle ridges comprise low sinuous ridges

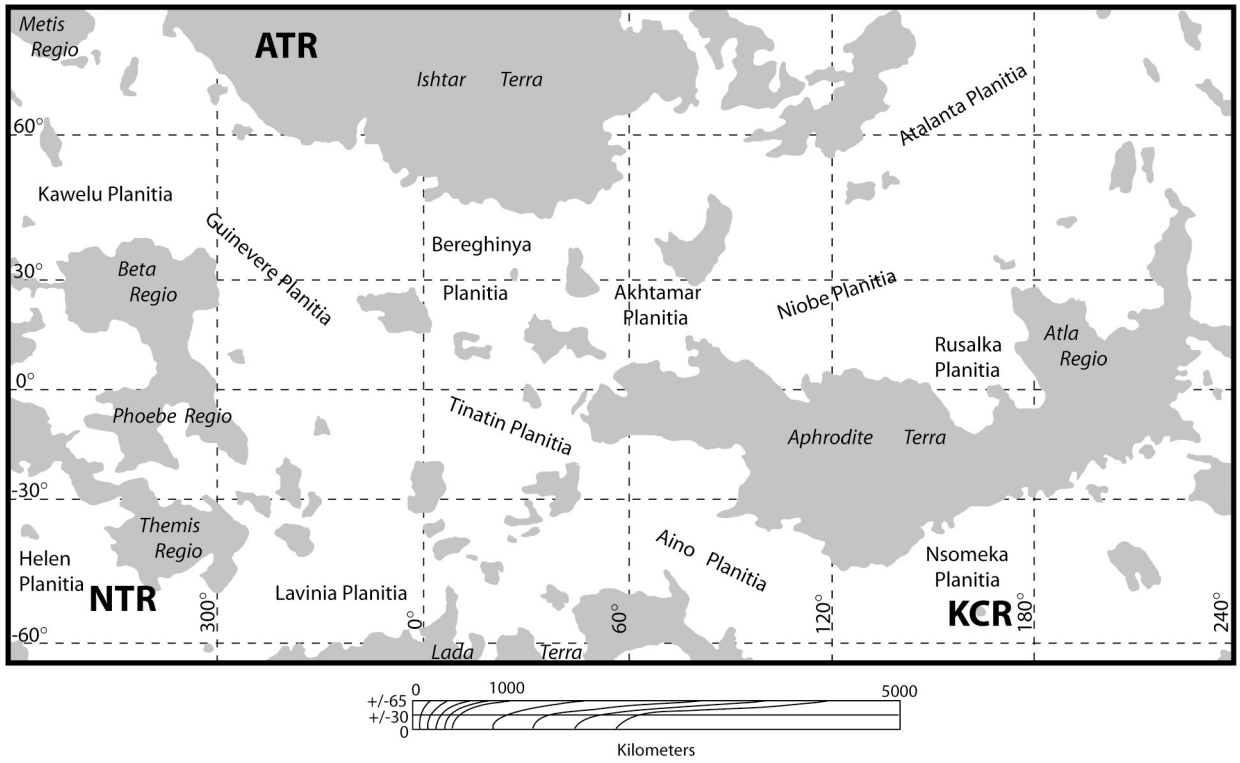

Figure 1. Sketch map of Venus in Mercator Projection showing the locations of the three field sites studied in this paper: (1) Norna Tessera region (NTR: 49°S, 268°E), (2) Kahlo Crater region (KCR: 58°S, 173°E), and (3) Atropos Tessera region (ATR: 68.5°N, 308°E). Gray regions represent highlands. After *Guest et al.* [1992].

tens to hundreds of kilometers long, 1–2 km wide, and hundreds of meters tall that record a small degree of regional contractional strain [*Plescia and Golombek*, 1986; *Watters*, 1988, 1991; *Golombek et al.*, 1991; *McGill*, 1993]. Low backscatter material in ATR lacks fractures and wrinkle ridges.

2.1. Data and Methodology

[7] Geologic mapping and channel analysis conducted in this research involved the use of S-band (12.6 cm wavelength) synthetic aperture radar (SAR) and altimetry data sets collected by the NASA Magellan mission. For a thorough review of the Magellan mission and experiments, see *Ford et al.* [1993]. Full-resolution SAR imagery has a resolution of 75–100 m/pixel. Magellan altimetry (~8 km along track and ~20 across track footprint [*Ford and Pettengill*, 1992; *Ford et al.*, 1993]) has a vertical resolution of better than 50 m [*Ford and Pettengill*, 1992]; the specific vertical resolution varies with latitude [*Ford et al.*, 1993]. All SAR images were viewed in both normal and inverted modes to highlight details of primary and secondary structures; structures are typically more apparent in inverted images. All SAR images presented herein are left-illuminated and inverted. For inverted SAR images, low backscatter areas appear bright and high backscatter areas appear dark. In addition, apparent illumination is reversed; hence left-illuminated inverted images appear right-illuminated. Magellan SAR imagery and altimetry are available at the U.S. Geological Survey Map-a-Planet Web site. Synthetic stereo views, created by merging SAR and altimetry [*Kirk et al.*, 1992] using NIH-Image macros developed by D.A. Young proved useful in elucidating geologic-topographic relationships. SAR interpretation follows *Ford et al.* [1993].

[8] Geologic mapping follows guidelines and cautions of *Wilhelms* [1990], *Tanaka et al.* [1994], *Hansen* [2000], and *Skinner and Tanaka* [2003]. With each study area, we mapped the region surrounding each channel in order to place the channel in spatial and temporal context. Robust quantification of channel depths in the three study areas is difficult with available SAR data and can, at best, be estimated based on apparent width:depth ratios; depths of channels appear to be much less than channel widths. On the basis of apparent width:depth ratios, we estimate channels in the three study areas to be on the order of meters to tens of meters deep. *Komatsu et al.* [1992] and *Oshigmai and Namiki* [2005] reached similar conclusions for the depth of Baltis Vallis using radar foreshortening measurements and radar backscatter models, respectively. In the process of mapping shields, we follow *Hansen* [2005] and rank shields by confidence levels: "definite shields" (obvious shields that most workers would be comfortable calling shields) and "potential shields" (possibly controversial features). Calculation of shield heights follows the methodology of *Guest et al.* [1992].

2.2. Study Area Geology

2.2.1. Kahlo Crater Region

2.2.1.1. Geologic Overview

[9] The Kahlo Crater region (KCR) (Figure 2) of southeast Nsomeka Planitia covers ~400,000 km^2; the study area

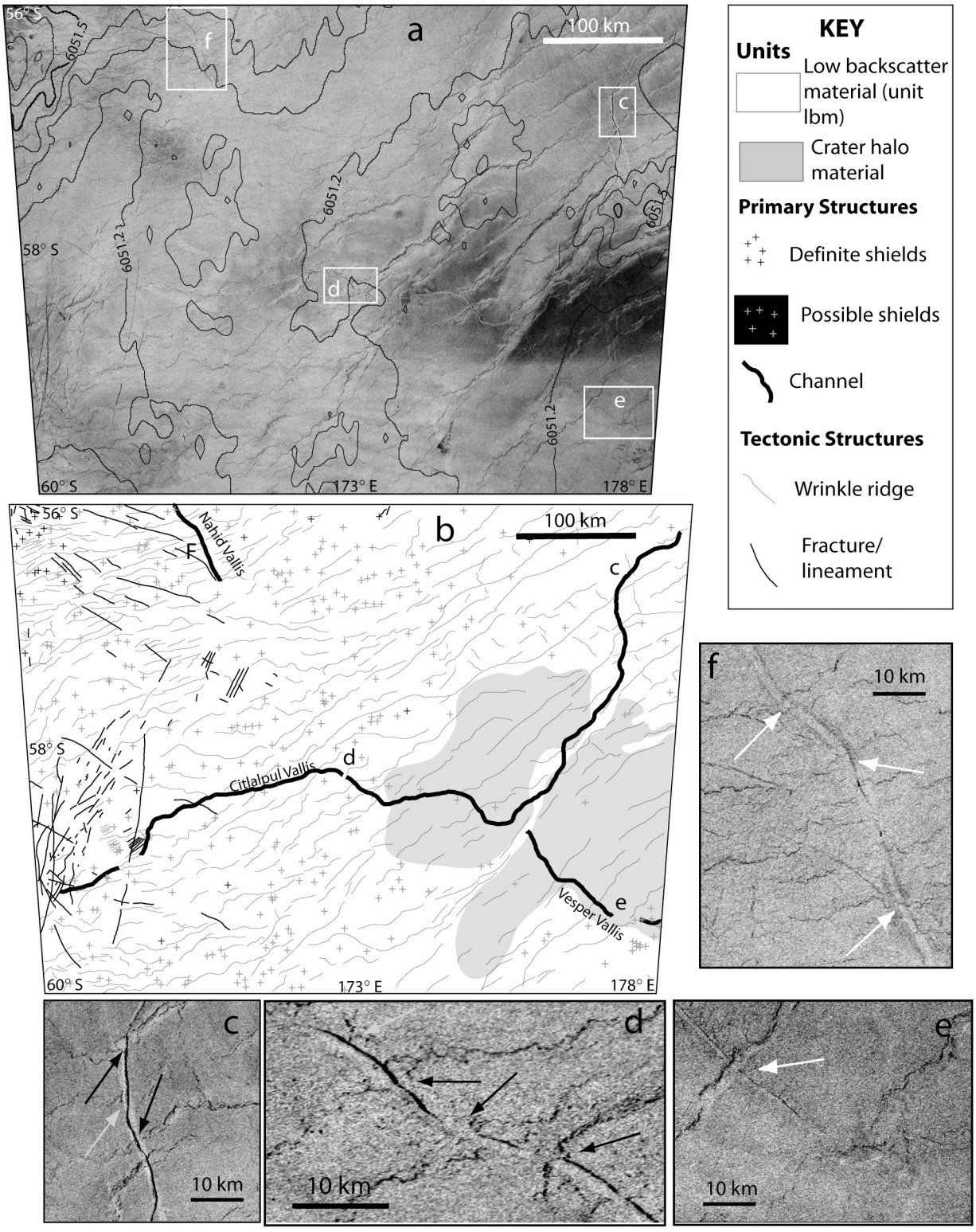

Figure 2. (a) Inverted synthetic aperture radar (SAR) image of the Kahlo Crater region shown with contoured altimetry data (contour interval is 100 m), white boxes surrounding c, d, e, and f show the locations of the c, d, e, and f insets: (b) Geologic map and (c–f) enlarged SAR images highlighting the three channel-wrinkle ridge relationships. White arrows highlight interaction type A (see text and Figure 3), black arrows highlight interaction type B, and gray arrows highlight interaction type C.

slopes gently to the southeast with a regional gradient of ~0.03°. Regional material shows dominantly a low radar backscatter character and hosts numerous shields. The regional material appears to be continuous within the study area and as such, we map it as unit lbm; unit lbm emplacement appears to be related to the numerous shields. Northeast-trending wrinkle ridges with wavelengths of <1–20 km locally deform unit lbm. North-trending fractures cut unit lbm in the western edge of the study area. The fractures may be genetically related to Fotla and Utset coronae, which lie outside the study area to the west and northwest, respectively. The eastern part of the study area includes high backscatter patches locally controlled by topography and possibly associated with the Kahlo impact crater located to the southeast of the study area.

2.2.1.2. Channel Description and Field Relations

[10] Segments of Citlalpul, Nahid, and Vesper Valles occur within the study area. All three channels occur within unit lbm. None of the channels exhibit distinct beginnings or termini.

[11] Citlalpul Vallis is ~400 km within the study area and broadly trends northeast with a constant width of approximately 1 km and an apparent depth on the order of tens of meters. The channel follows the regional topographic gradient until near 58.5°S, 176°E, where Citlalpul Vallis abruptly bends north and runs along topographic contour lines. An ~30 km long gap within Citlalpul Vallis occurs near 59°S, 170°E. Isolated radar bright lineaments ≪1 km wide and about 10–15 km long which parallel Citlalpul Vallis near 58.5°S, 172.5°E may represent channel levees.

[12] Nahid Vallis extends for ~40 km within the study area with a constant width of ~1 km and an apparent depth on the order of meters. The channel follows the regional topographic gradient and trends northwest. Isolated radar bright patches, possibly representing channel overflow material, ~2 km diameter and 10–20 km long extend alongside the margins of Nahid Vallis. Isolated radar bright lineaments ≪1 km wide and about 10 km long parallel Nahid Vallis near 56.2°S, 170.5°E, and may represent channel levees.

[13] Vesper Vallis extends for ~100 km within the field site with a constant width of approximately 1 km and a depth on the order of tens of meters. The channel follows the regional topographic gradient with the northwest end of Vesper Vallis located at the northeast bend of Citlalpul Vallis, suggesting a possible genetic relation between the two channels. An ~20 km long gap within Vesper Vallis occurs near 59.7°S, 177.5°E.

[14] Three distinct types of channel-wrinkle ridge interactions exist within KCR. These relationships are described below and illustrated in Figure 3.

[15] Interaction type A is highlighted by white arrows in Figures 2c, 2e, and 2f. A wrinkle ridge occurs up to, through, and on the other side of the channel as a complete entity; there is no interruption in the continuity of the ridge by the channel and the channel is deformed by the ridge. An imprint of the channel can be observed in cases where the wrinkle ridge is wide enough (Figure 2e).

[16] Interaction type B is highlighted by black arrows in Figures 2c and 2d. A wrinkle ridge ends at the margin of the channel and another wrinkle ridge also occurs with a similar trend on the opposite side of the channel margin such that the two ridges appear directly along trend from one another; a ridge segment is absent within the channel. The course of the channel is not influenced, impeded, or deflected by the presence of the ridges; the channel occurs immediately between the two ridges.

[17] Interaction type C is highlighted by gray arrows in Figures 2c and 2d. A wrinkle ridge ends at the channel margin and does not occur on the opposite side of the channel along trend; the ridge is absent within the channel. The path of the channel is not influenced, impeded, or deflected by the presence of the ridge; the channel-ridge intersection creates a "T."

[18] Citlalpul Vallis displays interactions A, B, and C, Nahid Vallis displays interaction type A, and Vesper Vallis displays interaction types A and B.

2.2.1.3. Geologic History

[19] Unit lbm is the oldest exposed unit within KCR and was likely emplaced via the numerous shields within the field site. The geologic history before emplacement of unit lbm is unconstrained. Unit lbm experienced regional contraction and possibly two periods of local extension subsequent to its emplacement. Timing between contraction and extension is unconstrained. The occurrences of the three channels within unit lbm suggest the channels formed either synchronously with or after, emplacement of unit lbm.

[20] Channel-wrinkle ridge interactions suggest multiple timing relations between the two feature types. For example, consider wrinkle ridges associated with interaction type A. Because the ridge continues as a complete entity across the channel and the channel appears deformed by the ridge, the channel must predate formation of the ridge. If the channel postdates the ridge, the channel should not exhibit deformation nor should the wrinkle ridge occur through the channel.

[21] Wrinkle ridges associated with interaction type B occur with the same trend on opposite sides of the channel, which implies that the ridges are genetically related and formed at the same time. If the ridges (and hence contraction) postdated the channel, the ridges should continue as a complete entity through the channel and the channel should exhibit deformation; that is, part of the wrinkle ridge should exist within the channel, or the channel should be uplifted along the wrinkle ridge (i.e., Figure 2e). Because ridges that show interaction type B do not deform or exist within the channels, the channels must either postdate interaction type B ridges or overlap in their timing with ridge formation, similar to the development of terrestrial antecedent drainages [e.g., *Burbank et al.*, 1996; *Bloom*, 1998]. Therefore interaction type B ridges are either older than or formed synchronously with, channels in KCR.

[22] The timing between interaction type C wrinkle ridges and channels is ambiguous. It is possible that the channel served as a free surface that blocked propagation of the younger ridge [*Engelder and Geiser*, 1980; *Pollard and Aydin*, 1988; *Price and Cosgrove*, 1991], which would infer that the channel is older than the ridge. However, it is also conceivable that the channel serendipitously formed at the edge of a preexisting wrinkle ridge. Hence interpretations of the timing relationships represented by interaction type C are ambiguous.

[23] On the basis of the above arguments, Nahid Vallis predates formation of the local wrinkle ridges, whereas

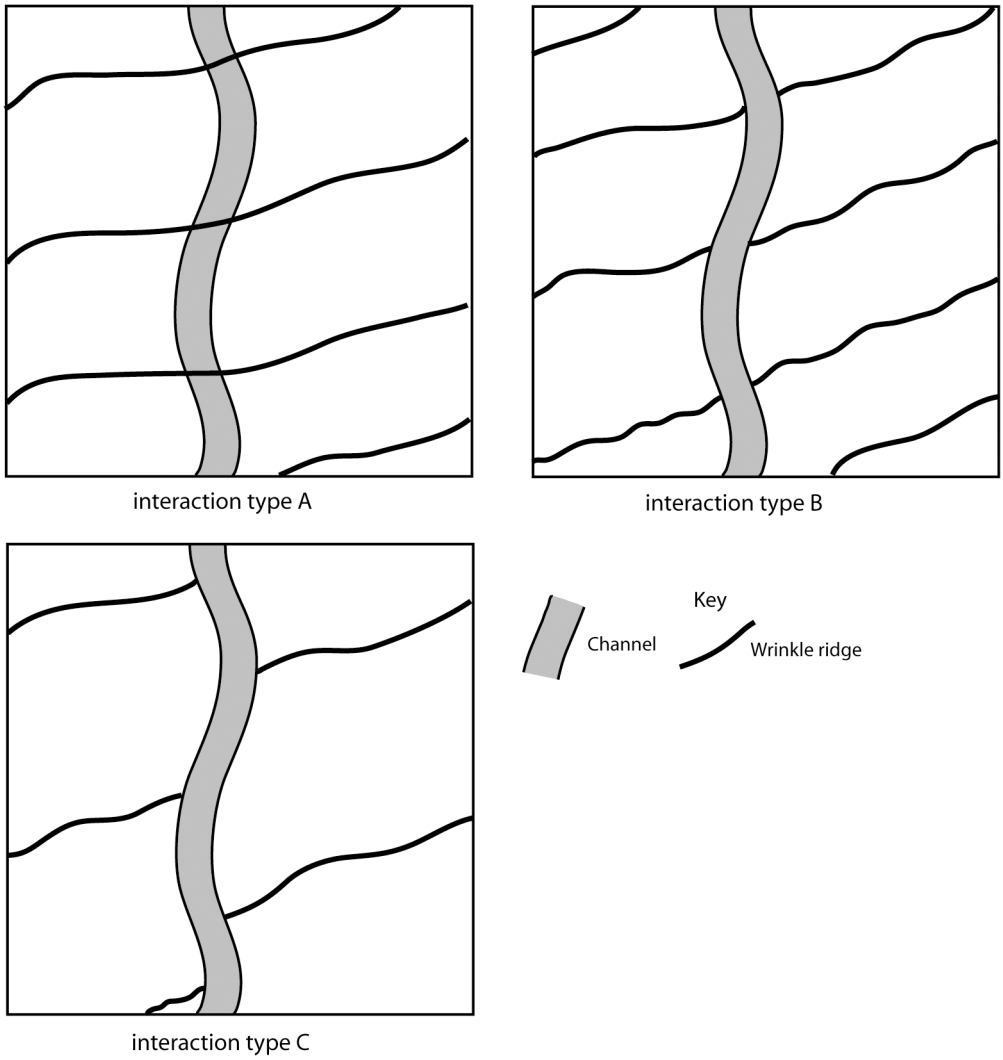

Figure 3. Cartoon maps illustrating the three types of channel-wrinkle ridge interactions noted in the KCR field site. Interaction type A: Wrinkle ridges occur up to, through, and across the channel as complete entities; there is no interruption in the continuity of the ridges by the channel and the channel is ultimately deformed by the ridge. An imprint of the channel can be observed in cases where the wrinkle ridge is wide enough (see Figure 2e). Interaction type B: Wrinkle ridges end at the margin of the channel and then continue with the same trend on the opposite side of the channel margin such that the ridges appear that they should connect across the channel; ridges are absent within the channel. The course of the channel is not influenced, impeded, or deflected by the presence of the ridges. Interaction type C: Wrinkle ridges end at the channel margin and do not continue on the opposite side of the channel margin; ridges are absent within the channel. The course of the channel is not influenced, impeded, or deflected by the presence of the ridges.

Citlalpul and Vesper Valles each display a time transgressive relation with their local wrinkle ridges.

2.2.2. Norna Tessera Region

2.2.2.1. Geologic Overview

[24] The Norna Tessera region (NTR) (Figure 4) of southeast Helen Planitia is an ~200,000 km^2 study area that slopes to the south with a regional gradient of ~0.15°. Within NTR, kipukas of tessera terrain [*Basilevsky et al.*, 1986] associated with Norna Tessera and a basal terrain peak through a local cover of low backscatter material. The low backscatter material appears to be continuous and hosts numerous shields and associated deposits and as such we map it as unit lbm; unit lbm emplacement appears to be related to the numerous shields. Basal terrain is defined as material(s) that hosts at least one suite of tectonic structures marked by tightly spaced ($\ll$1 km spacing) lineaments, which have destroyed the character of the original unit(s) [*Wilhelms*, 1990]. The tessera terrain hosts north-northwest-trending ribbon structures [*Hansen and Willis*, 1998] (wavelengths 1–3 km) and northeast-trending lineaments (spacings <1–10 km). Northwest- and local northeast-striking fractures with spacings of <1–10 km cut the basal terrain. Broad arcuate warps and local northwest- and northeast-striking fractures with spacings of 1–10 km associated with

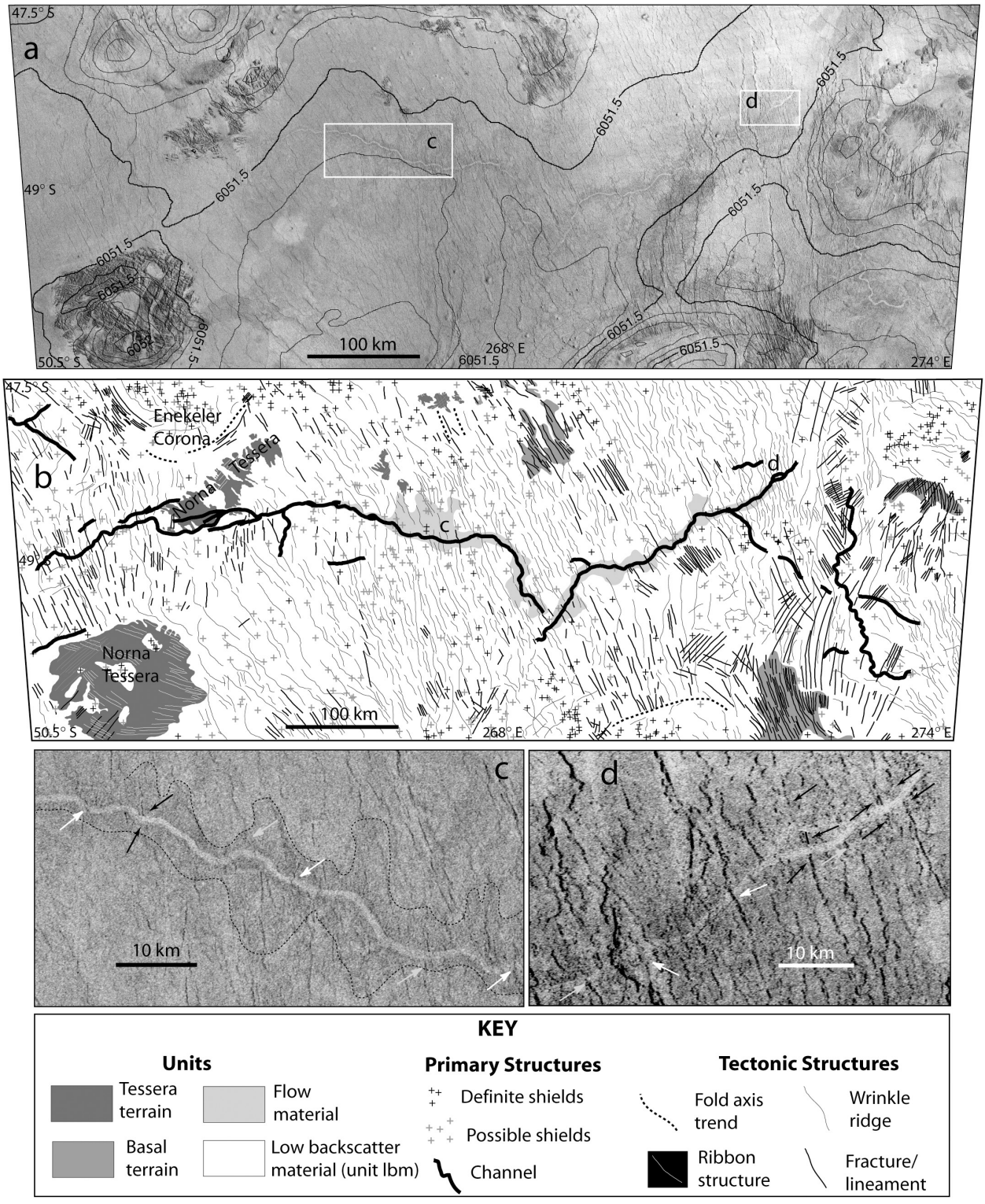

Figure 4. (a) Inverted SAR image of the Norna Tessera region shown with contoured altimetry data (contour interval is 100 m), white boxes surrounding c and d show the locations of the c and d insets; (b) geologic map, and (c,d) enlarged SAR images highlighting the three channel-wrinkle ridge relationships. White arrows highlight interaction type A, black arrows highlight interaction type B, and gray arrows highlight interaction type C. Dashed lines in c represent the outline boundaries of high backscatter material that occurs along two segments of Sinann Vallis.

Enekeler Corona extend into the northwestern part of the study area. The fractures locally cut unit lbm, which in turn, locally covers the fractures. Unit lbm embays both tessera terrain and basal terrain resulting in a complex and tight digitate contact inferring a low angle boundary between the two basal terrain units and the stratigraphically higher unit lbm. The complex contact also indicates that unit lbm is a thin unit, an interpretation consistent with *Guest et al.* [1992], who estimated shield associated deposits as likely tens of meters or less in thickness (see also, *Hansen* [2005]). On the basis of the consistency of structural trends between spatially separate tessera terrain and basal terrain, tessera and basal terrain units most likely extend in the subsurface below unit lbm.

2.2.2.2. Channel Description and Field Relations

[25] Sinann Vallis consists of several disconnected channel traces that occur within unit lbm across the field site with a total length of >1000 km. Most segments trend east-west and broadly run along topographic contour lines, although one segment in the eastern part of the map area follows the local topographic gradient. Channel segments maintain a consistent width of approximately 1 km, although some segments narrow to a width of <1 km. All segments appear to be on the order of meters to tens of meters deep. No channel traces in the map area contain distinct beginnings or termini. Intermediate backscatter material, possibly representing overflow deposits from the channel, forms a band with varying widths of 1–10 km that parallels parts of the two long segments of Sinann Vallis in the central part of the field site.

[26] The three types of channel-wrinkle ridge interactions documented in KCR also exist within NTR (Figures 4c and 4d).

2.2.2.3. Geologic History

[27] Tessera terrain and basal terrain represent the two oldest units inferred by embayment relations. Temporal relations between the two units are unconstrained given that the units are never in contact with one another. Unit lbm locally postdates both tessera terrain and basal terrain. Although unit lbm locally covers fractures of basal terrain, parallel fractures also cut the low backscatter material, indicating either a time transgressive relation or fracture reactivation subsequent to unit lbm emplacement. Wrinkle ridges deform and therefore postdate the emplacement of unit lbm. Similar to the channels in KCR, the occurrence of Sinann Vallis within unit lbm implies that the channel either formed either synchronously with or after, emplacement of unit lbm. The occurrence of channel segments that follow topographic contour lines suggests the possibility that regional tilting occurred after channel formation, although the possibility that forces other than the topographic gradient (i.e., gravity) drive fluid flow cannot be excluded. Following timing arguments outlined for channel-wrinkle interactions in KCR, interaction type A wrinkle ridges must postdate Sinann Vallis, interaction type B ridges either predate or overlap in their timing with Sinann Vallis, and interaction type C wrinkle ridges have an indeterminable temporal relation with the channel. Therefore Sinann Vallis has a time transgressive relationship with wrinkle ridges.

2.2.3. Atropos Tessera Region

2.2.3.1. Geologic Overview

[28] The Atropos Tessera region (ATR) (Figure 5) of western Ishtar Terra includes ~160,000 km^2 that slopes down to the west-southwest with a gradient of approximately 0.1°. ATR consists of inliers of folded ribbon terrain [*Hansen and Willis*, 1996, 1998] associated with Atropos Tessera; folds within Atropos Tessera trend northwest with wavelengths of 30–40 km. In the northwestern part of the study area, Atropos Tessera grades into numerous kipukas that reflect northwest fold trends. Ribbon structures trend dominantly north-northeast with wavelengths of 1–3 km, although local northwest trends occur. A local low backscatter material that hosts numerous shields and mapped as unit lbm embays local topographic lows within the folded-ribbon tessera terrain; unit lbm emplacement is likely associated with the numerous shields. The contact between unit lbm and tessera terrain makes a complex and tight digitate boundary inferring an extremely shallow contact with the stratigraphically higher unit lbm comprising a thin layer. Following the thickness arguments for NTR, unit lbm also appears to represent a thin unit in ATR. A suite of northeast-trending wrinkle ridges with wavelengths of 1–10 km deform unit lbm in the southeast part of the field site. Impact ejecta from Ivka crater extends into the western edge of the study area.

2.2.3.2. Channel Description and Field Relations

[29] Lunang Vallis is an approximately 200 km long channel that follows a synclinal axis within Atropos Tessera. Lunang Vallis occurs within unit lbm, follows the regional topographic gradient, and appears to originate from a 5 km wide circular depression, or pit. The pit forms part of a sinuous pit chain in the southeast corner of the field site. No flow material appears to surround the beginning of the channel, although a halo of material that possibly reflects extruded material surrounds one pit (highlighted by double-barred arrow in Figure 5d) suggesting the pit chain is the surface expression of a subsurface conduit that transported fluid. The main trunk of Lunang Vallis has a width of approximately 1 km and appears to be on the order of tens of meters deep; near 307.8°E, 68.4°N the trunk narrows to where it either ends or continues below effective image resolution as defined by *Zimbelman* [2001]. A mixture of low and high backscatter material, possibly representing deposited channel material, surrounds the channel as it narrows and disappears near 68.5°N, 307°E. Near 68.3°N, 308°E, distributary channels break from the trunk channel and form what appears to be a braided channel system. The distributaries are <1 km wide and extend for about 30 km. An additional channel 1 km wide is located about 10 km south of Lunang Vallis. This second channel also originates from a pit near 68.2°N, 309.5°E and extends nearly 30 km before either ending or continuing below effective image resolution. No levees are observed along the length of Lunang Vallis.

[30] Between 68.4°N, 308.5°E and 68.3°N, 309.5°E, a series of quasi-circular topographic highs (approximately tens of meters tall) occur immediately alongside the margins of Lunang Vallis (highlighted by black arrows in Figures 5c and 5d). On the basis of their quasi-circular nature, we interpret these topographic highs as remnants of shield edifices where the shield margin alongside Lunang Vallis may reflect eroded parts of the edifice. Some shield remnants occur on opposite sides of Lunang Vallis whereas other remnants occur only on one side of the channel. It is easy to envision that remnants that occur on opposite margins of the channel are genetically related and were

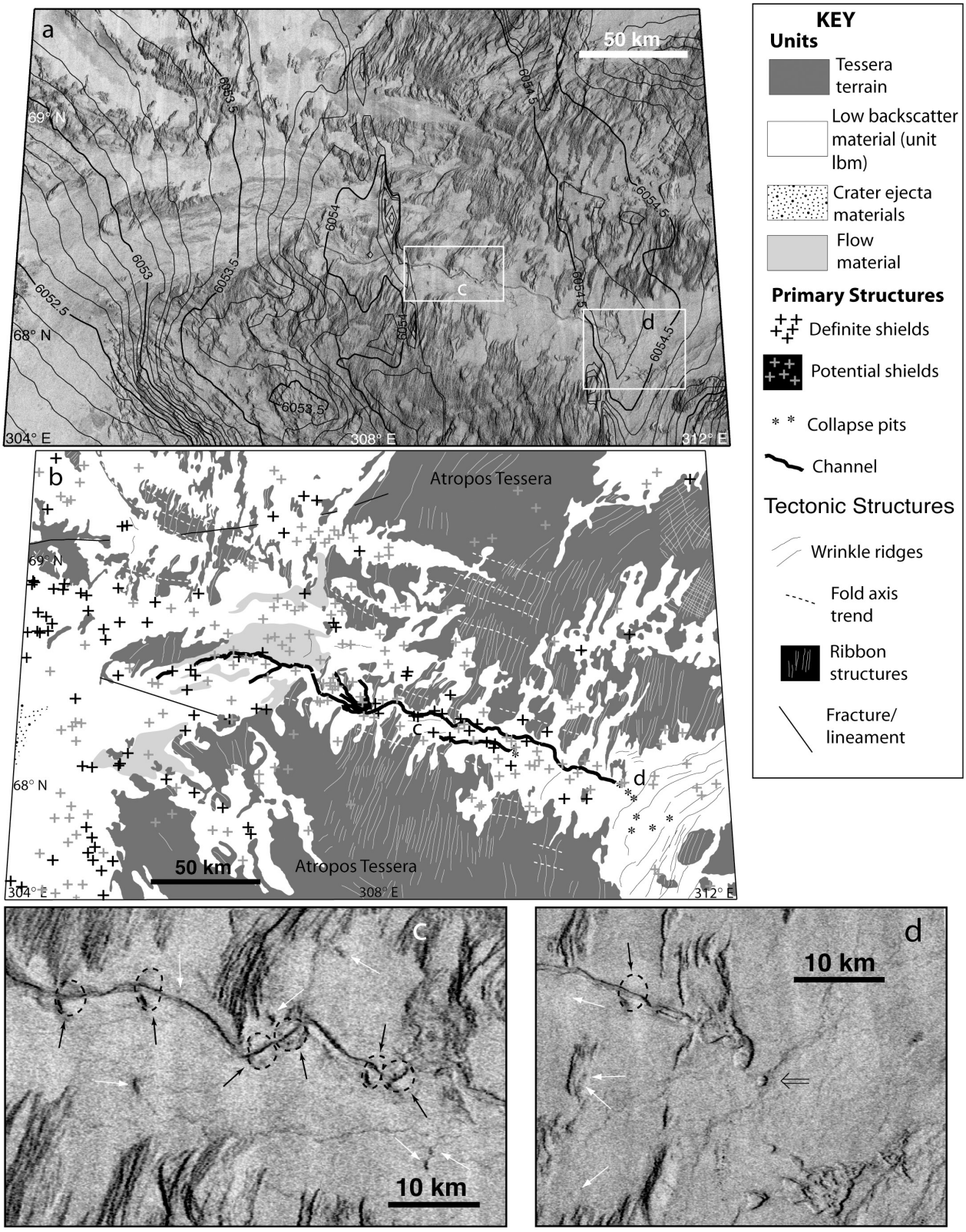

Figure 5. (a) Inverted SAR image of the Atropos Tessera region shown with contoured altimetry data (contour interval is 100 m), white boxes surrounding c and d show the locations of the c and d insets; (b) geologic map; (c, d) enlarged SAR images highlighting the channel-shield relationships observed in ATR. Black arrows highlight the locations of the erosional remnants of shield edifices and dashed black circles represent the outlines of reconstructed shield edifices; white arrows highlight intact shield edifices; double-barred arrow in d highlights flow material that surrounds a pit near the beginning of Lunang Vallis.

once connected to form a single shield edifice; black circles in Figures 5c and d represent reconstructed shields; reconstructed shields have diameters of about 1–2 km, which is larger than most other shield edifices mapped in the field site.

[31] The relationship between the shield remnants and Lunang Vallis is similar to interaction type B (see Figure 3) observed in the KCR and NTR field sites, except that the topographic highs in this case are shield edifices and not ridges. Lunang Vallis is not diverted by any shield remnants. Although the channel does exhibit a meandering nature, the meanders appear to be unrelated to the presence of the shields.

2.2.3.3. Geologic History

[32] On the basis of embayment relations, tessera terrain represents the oldest exposed unit in ATR. The consistency of structural trends within the tessera terrain suggests that it extends across part of the map area beneath the stratigraphically higher unit lbm. Ivka crater locally postdates the low backscatter material. Similar to the other two study areas, the occurrence of Lunang Vallis within unit lbm suggests the channel formed either synchronously with or after, unit lbm emplacement. The presence of shield remnants along the margin of Lunang Vallis implies that at least some stage of channel activity postdated shield formation; if the shields postdated Lunang Vallis, then the shields should locally cover the channel.

3. Discussion

3.1. Channel Analysis

[33] Despite their widely separate locations, channels within the three study areas share several characteristics. (1) Channels occur completely within a low backscatter material (unit lbm) that appears to form a thin veneer across each field site. (2) Channels maintain mostly consistent widths along their lengths. (3) With the exception of Lunang Vallis, channels do not have any obvious beginning or termini; Citlalpul, Vesper, and Sinann Valles also include disconnected traces. (4) Channel bottoms appear to be topographically lower than surrounding unit lbm (i.e., channels appear to be negative topographic features). (5) Some channels are associated with possible lateral flow deposits and levees, although these appear to be local and isolated occurrences; the beginning of Lunang Vallis is not associated with any obvious lateral flow deposits. (6) Channels dissect topographic highs including wrinkle ridges and shields (i.e., interaction type B) with no deflection in the channel course. Any model of channel formation within the three study areas must address the above six characteristics.

[34] Because previous hypotheses of channel formation carry the assumption of channel formation as a surface process, it seems logical to try to explain channel formation in our three study areas through surface fluid flow. However, the presence of dissected topographic highs (i.e., interaction type B) seems inconsistent with surface fluid flow, and requires further explanation. The interaction between a topographic high and a fluid flowing across the surface will result in a predictable sequence of events. For example, a fluid flowing across the surface should respond to preexisting surface topography. That is, preexisting surface topography should influence the course of the fluid. Topographic highs should either deflect the course of the fluid, and hence the path of the channel, or stop fluid movement such that the fluid accumulates along or follows the margin of the topographic high. No such observations exist for any channel-topographic high interaction in the three study areas; in fact, channels in the three study areas clearly dissect topographic highs.

[35] However, if the channel existed prior to formation of the topographic high and was active throughout formation of the high, an antecedent drainage may develop [e.g., *Burbank et al.*, 1996; *Bloom*, 1998] resulting in the interaction type B relation. The creation of an antecedent drainage is controlled by the relation between the rate of formation of the topographic high and the fluid incision rate [*Burbank et al.*, 1996]. In the case of KCR and NTR, the formation rate of topographic highs is the uplift rate of wrinkle ridges, whereas in ATR, it is the formation rate of shields.

[36] Interaction type B relations noted in KCR and NTR appear similar to terrestrial antecedent drainages [e.g., *Bloom*, 1998], perhaps suggesting a similar process of formation. No temporal constraints exist for the uplift rate of wrinkle ridge on Venus, but uplift rates for features on the Columbia Plateau analogous to Venusian wrinkle ridges [*Mege and Ernst*, 2001] are calculated to be less than 0.2 mm/yr [*Reidel et al.*, 1980]. Assuming a similar uplift rate for Venusian wrinkle ridges, uplift of a 100 m high wrinkle ridge (possibly a small to medium sized wrinkle ridge based on estimated heights [*Plescia and Golombek*, 1986; *Watters*, 1988, 1991; *Golombek et al.*, 1991]) would take 50,000 years, requiring channel systems in KCR and NTR to remain continuously active for greater than 50,000 years. This is geologically reasonable if the channel is a fluvial system carved by water [e.g., *Bloom*, 1998], but it does not seem reasonable if the carving fluid is lava. Although some lavas, such as carbonatite, have documented erosion rates as fast as 2 mm/min [*Dawson et al.*, 1990] into a substrate of their own material, it does not seem geologically reasonable that a lava channel system will remain active with continuous flow for 50,000 years. To do so would require prolonged eruption periods unlike any documented on Earth. Thus an antecedent interpretation for channel-topography interactions requires that such magma generation and lava flow processes be addressed.

[37] Lunang Vallis in ATR provides a slightly different antecedent drainage scenario in which the channel intersects shield edifices instead of linear ridges. Because the eroded margins of the shield edifices occur immediately alongside Lunang Vallis, it seems likely that Lunang Vallis was directly involved in erosion of the edifices; Lunang Vallis appears to have dissected the middle of the edifices. If Lunang Vallis formed by fluid flow on the surface, then the observation of dissected shield edifices requires that several volcanic centers formed immediately on top of a preexisting Lunang Vallis. Lunang Vallis must have then been active and remained active throughout formation of the shield while simultaneously downcutting through the center of active volcanic edifices. This required scenario is inconsistent with both observations and geologic reasoning. Even if Lunang Vallis downcut through the shields at rates equal to or faster than shield formation, shield eruptions should

theoretically divert fluid in the channel such that the channel bends around the edifice and erupted deposits; no such diversions are observed. In addition, it is unclear how the shield edifice could form with an apparent cone-shaped morphology while a river ran through.

[38] Hence channel-wrinkle ridge interactions in KCR and NTR and channel-shield interactions in ATR are difficult to explain within the context of an antecedent hypothesis.

[39] Perhaps channel formation may be due to lava tube processes. A lava tube hypothesis would explain the disconnected segments of some channel segments, the apparent negative topographic appearance of channels, and the localized occurrences of lateral flow deposits and levees. Further, lava tube processes could possibly explain the channel-shield relationships in Lunang Vallis. As some of the shields in ATR formed directly over the trace of Lunang Vallis, it is possible that Lunang Vallis and the shields are genetically related. To illustrate, shield edifices termed "rootless shields" occur above some lava tubes and likely result from the eruption of tube lava through the solidified tube cover and onto the surface [*Kauahikaua et al.*, 2003]. Shield remnants along Lunang Vallis could reflect a similar process in which the volume of material moving through a roofed over channel exceeds the conduit volume resulting in the "eruption" of tube fluid at the surface creating the shield edifice. After draining of the tube, the rootless shield collapses into the channel resulting in the current channel-shield relation. By the lava tube scenario, however channels would have formed by marginal cooling of a larger lava flow that created a central channel [e.g., *Hulme*, 1974] that facilitated continued lava transport, and eventually formed a roof to create a tube [e.g., *Hon et al.*, 1994; *Dragoni et al.*, 1995]. As each channel occurs within unit lbm, unit lbm must comprise the larger lava flow whose margins cooled to form the channels; unit lbm must therefore consist of a single flow unit. However, map relations suggest that unit lbm does not consist of a single lava flow. Instead, it is composed of numerous flow units sourced from individual shields and has a history separate from Lunang Vallis. Furthermore, the dissected wrinkle ridges place the same volcanic activity constraints on the lava tube hypothesis as on surface fluid flow hypothesis. Assuming the same uplift rate as before for a 100 m high wrinkle ridge, the lava tube system would have to remain active with continuous flow for more than 50,000 years again requiring explanation for such magma generation and lava flow processes. Consequently, map relations and current geologic reasoning are inconsistent with channels in the three study areas forming as a lava tube.

[40] As a third alternative, maybe channel formation can be attributed to the movement of fluid in the subsurface by a process similar to piping that occurs in clastic, nonsoluble materials [e.g., *Parker et al.*, 1990]. In piping [*Parker et al.*, 1990; *Jones*, 1990], water either percolates down through a permeable layer or follows a preexisting structure to an impeding horizon, which facilitates lateral transport of the water along a gradient. Movement of the water along the impeding horizon induces mechanical erosion of surrounding material to create a conduit that allows more movement of fluid through the system [*Parker et al.*, 1990]. Erosion may eventually reach the surface resulting in piecemeal exposures of the subsurface conduit. Continued erosion may result in the eventual connection of the exposures, creating a continuous channel that may display meanders [*Jones*, 1990] and may not have any distinct beginnings or termini [*Parker et al.*, 1990]. Ultimately, the fluid traveling in the subsurface does not "see" surface topography and carves overlying materials without regard for surface topography. Subsurface fluids travel independent of surface morphology and can potentially cut through topographic surface features such as ridges. Channels created by piping can also display variable sizes. Channel depths and diameters range from centimeters to tens of meters and lengths range from meters to hundreds of meters [*Parker et al.*, 1990; *Jones*, 1990]; the depth to the impeding horizon dictates the depth of the piped channels [*Parker et al.*, 1990]. Piping differs from lava tube formation in that lava tubes are constructional features built by the cooling and crystallization of lava whereas piping tubes are created by fluid movement eroding surrounding materials to create a conduit. Despite the differences in size, features created by piping processes are analogous to the characteristics of channels in the three study areas. It then seems plausible that the channel in this study formed by processes at least similar to piping. Maybe channel formation in our three study areas represents a volcanic variation of piping on Earth where lava flow between an impeding horizon and an overlying "permeable" layer facilitates erosion of surrounding materials. Such a mechanism for channel genesis is consistent with all of the listed characteristics of channels in our study areas. Particularly, the conduit lava may erode to the surface possibly dissecting preexisting topographic highs that reside above the conduit such as ridges and shield edifices. The resulting channel would then appear as a negative topographic feature and, depending upon the degree of upward erosion, may appear as a series of disconnected traces. In addition, since the channel results from lava carving up, lateral flow deposits would be absent, unless the lava periodically overflowed the channel margins. Finally, the beginnings and termini of channels may remain unexposed in the subsurface simply due to the lava having not fully eroded to the surface in these locations. Hence the formation of channels in the three study areas seems easily accommodated into a piping-like origin.

3.2. What Is the Low Backscatter Material?

[41] Low backscatter material (unit lbm) is the most aerially expansive geologic feature in each study area. Although abundant shields and associated deposits characterize low backscatter material, their origin is uncertain. *Hansen* [2005] may provide an explanation. *Hansen* [2005] described a 10,000,000 km^2 region north of Aphrodite Terra [see *Aubele*, 1996] that has characteristics similar to low backscatter materials in our three study areas. To illustrate, *Hansen*'s [2005] study area, which consisted of Sogolon, Niobe, and Llorona Planitiae, hosts tens to hundreds of thousands of shields that do not describe any discernable patterns across the entire region and are not associated with any larger-scale volcanic feature. Furthermore, shield associated deposits coalesce to form a layer termed "shield paint" that is approximately meters to tens of meters thick and forms apparently shallow contacts with stratigraphically lower units. *Hansen* [2005] termed such a shield-dominated occurrence "shield terrain" and hypothesized that it reflects

in situ partial melting of basaltic crust. Partial melting of basalt will produce a melt product that is more felsic and hence has a lower melting temperature than basalt [*Winter*, 2001]; melt residuum may then have a higher melting temperature than basalt. The formation of shield terrain may have occurred across Venus's history [*Hansen*, 2005]. Although *Hansen* [2005] described shield terrain only north of Aphrodite Terra, *Stofan et al.* [2005], in a study of resurfacing styles in 18 Venusian quadrangles, noted regions on other parts of Venus with large abundances of shields. It is plausible then that shield terrain is more extensive on Venus than documented by *Hansen* [2005] and that the low backscatter material in our three study areas mapped as unit lbm may represent shield terrain. Channels in our three study areas may therefore form in shield terrain.

4. Stoping Hypothesis of Channel Formation

[42] On the basis of our descriptive analysis of channels in three widely separate study areas and the easy accommodation of channel characteristics into a subsurface origin, we propose a new hypothesis of channel formation, the stoping hypothesis (Figure 6), which we infer as a volcanic variation of piping processes on Earth [e.g., *Parker et al.*, 1990]. Lava travels along an interface in the subsurface where it erodes or stopes overlying material resulting in the formation of a subsurface conduit. Continual fluid movement may cause erosion and stoping that eventually reaches the surface independent of preexisting topographic highs such as wrinkle ridges and shields. Further stoping can eventually result in the coalescence of the discontinuous segments creating a continuous channel. Upward erosion would ultimately undermine any preexisting topographic highs located above the conduit resulting in interaction type B relations. Once the conduit is exposed to the surface, it becomes a channel where lava would most likely continue to flow insulated by the CO_2-rich atmosphere [*Snyder*, 2002] and the formation of any local surface crust [e.g., *Greeley*, 1971] or roof [e.g., *Hon et al.*, 1994; *Dragoni et al.*, 1995]. The conduit, or channel, may occasionally overflow locally depositing flow material and/or build levees along the channel margins. After draining of the channel, parts of the insulating crust and/or roof may remain, hiding the channel from surface view providing another explanation for the origin of segmented traces of some channels, as observed. The consistent widths of channels suggests that the physical properties of the substrate [*Wohl and Achyuthan*, 2002], the dynamic behavior of lava within the channel, and the slope on which the lava flowed all remained constant along the lengths of the channels. Any time after establishment of a conduit, lava tube-type processes could occur. For example, as discussed earlier for Lunang Vallis, unsteady supply rates of fluid within the subsurface conduit, may result in the eruption of material to the surface building ''rootless shields'' [*Kauahikaua et al.*, 2003]. In addition, a subsurface conduit will insulate lava more so than the presence of a crusted roof on an open channel flow [*Keszthelyi*, 1995; *Sakimoto and Zuber*, 1998; *Harris et al.*, 2005], which may serve to further enhance the occurrence of thermal erosion.

[43] Topographic gradients and/or pressure gradients may drive fluid movement along the interface and the mode of erosion may be mechanical, thermal, or thermomechanical depending upon the physical and chemical properties of the lava and surrounding material. The stoping hypothesis makes no specific predictions as to the type of lava involved in channel formation; in fact, a wide range of lavas could be a candidate. Clearly, the nature of the suprastrate and substrate, which are equally unknown, must also be considered. If the low backscatter materials (suprastrate) represent a felsic partial melt of basalt, then lava more mafic than the low backscatter materials should be able to thermally erode the suprastrate meaning that thermal erosion, or at least thermomechanical erosion [e.g., *Fagents and Greeley*, 2001], may be responsible for the formation of the conduit and subsequent channel. Hence basalt could theoretically carve the conduits that evolve into the channels in this study. If the basal layer has a basaltic composition (as presumed), then basalt lava could thermally erode the low backscatter materials, but it would not substantially erode the basal materials [e.g., *Keszthelyi*, 1995; *Sakimoto and Zuber*, 1998; *Fagents and Greeley*, 2001] meaning that the basal materials serve as the lava substrate. The ''permeable'' layer in piping processes on Earth is then the thermally erodible layer in the stoping hypothesis; the local basal materials represent the impeding horizon. As a result, fluid flow and subsequent conduit-channel formation in the stoping hypothesis is concentrated at the subsurface boundary between the low backscatter materials mapped as unit lbm and stratigraphically older basal materials. This predication is consistent with the thickness of unit lbm and the depths of channels in the three study areas, which appear to be on the order of meters to tens of meters. Therefore the thickness of the low backscatter material dictates channel depth.

[44] The presence of subsurface structures will not impede processes of conduit-channel formation in the stoping

Figure 6. Cartoon block diagrams outlining an alternative hypothesis for Venusian channel formation, which we term the stoping hypothesis. Curved dashed lines with question marks along cross-sectional views of the block diagram represent the possible merging of the subsurface structure of wrinkle ridges into a decollement at the base between unit lbm (light colored layer) and stratigraphically older basal materials (dark colored layer). In block *t*0, surface materials (light colored layer) rest unconformably on local basement materials (dark colored layer). In block *t*1, fluid moves in the subsurface along the interface between the two layers. Fluid flow forms a conduit via erosion of surrounding surface materials. The type of fluid is unconstrained, and erosion could occur by thermal or mechanical processes, or both. However, on the basis of arguments in the text, basalt may carve the channels through largely thermal and thermomechanical processes. In block *t*2, continued movement of the fluid through the conduit continues to erode the overlying surface materials, resulting in discontinuous exposures of the conduit at the surface. Fluid may overflow from the exposed conduit, or channel, onto the surface, creating levees and depositing flow material along the channel margins. Block *t*3 shows that eventually, all overlying material is eroded, resulting in an open and continuous channel segment. The depth of the channel is dictated by the depth to basal materials (see text for more discussion).

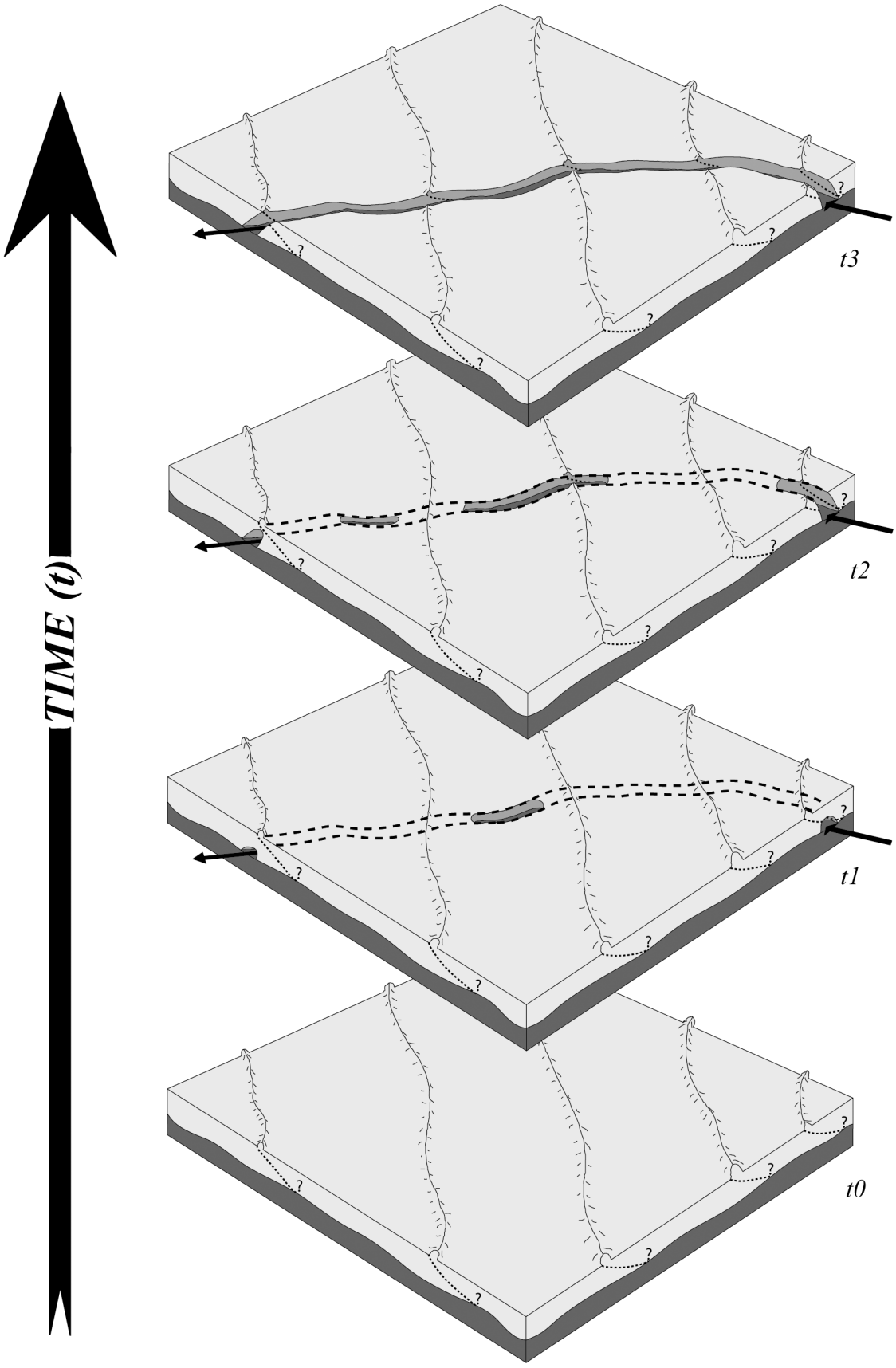

Figure 6

hypothesis. For example, we infer that wrinkle ridge-related deformation is confined to unit lbm where wrinkle ridges possibly shallow to a decollement at the boundary between unit lbm and stratigraphically older basal materials [e.g., *Lutter et al.*, 1994]. Therefore the subsurface extension of a wrinkle ridge in the low backscatter materials only juxtaposes unit lbm against unit lbm. The fluid thermally eroding unit lbm will not "see" the juxtaposition because unit lbm is set against itself; the physical properties of the deformed material are the same on either side of the subsurface structure. However, the thickness of the mechanical layer deformed by wrinkle ridges is ultimately unconstrained [*Mege and Ernst*, 2001, and references therein] and detailed discussion of wrinkle ridge formation is nontrivial and beyond the scope of the current contribution.

[45] The idea of subsurface fluid movement eroding overlying material on Venus is not new. *Komatsu et al.* [2001] postulated that valley networks on Venus formed by subsurface movement of fluid along preexisting tectonic structures that sapped overlying material. Although our hypothesis does not call upon structural control of fluid movement, the spirit of the stoping and sapping hypotheses is similar. Together, these two hypotheses suggest that the movement of subsurface fluid may play a larger role in shaping the Venusian surface than previously recognized. Considering recent studies on Earth and Mars that demonstrate subsurface rather than surface processes may adequately explain various geomorphic features such as pirated streams [e.g., *Pederson*, 2001] and Martian gullies [e.g., *Marquez et al.*, 2005, and references therein], entertaining hypotheses of fluid flow in the shallow crust on Venus seems justified. However, we do not suggest that the stoping hypothesis applies to the formation of all Venusian channels. The stoping hypothesis may be just one of many mechanisms of channel formation on Venus [e.g., *Gregg and Greeley*, 1993; *Bussey et al.*, 1995]. That is, channels might not be created equally.

5. Summary and Conclusions

[46] Our analysis of three widely separated study areas questions the fundamental assumption that Venusian channel formation is a surface process. The three study areas host channels that dissect preexisting topographic highs with no deflection in the channel course. This relationship is difficult to reconcile with surface fluid movement. Instead, we propose the stoping hypothesis where at least some Venusian channels form by the subsurface movement of fluid along an interface between low backscatter surface materials (unit lbm) and basal materials. Fluid movement will facilitate piecemeal stoping and erosion of the overlying materials ultimately resulting in the surface exposure of a continuous channel. The overlying low backscatter material in each study area is abundant with shield edifices and resembles shield terrain of *Hansen* [2005], which may represent a felsic partial melt differentiate of basalt. The stoping hypothesis makes no predictions as to the channel forming fluid, although lava as common as basalt may carve the channels. Ultimately, the stoping hypothesis is a volcanic variation of piping processes on Earth in that lava, instead of water, flows along an impeding horizon in the shallow subsurface that is capped by a thermally erodible, instead of a permeable, layer. Lava flow along the interface will thermally, or possibly thermomechanically, erode overlying materials. The stoping hypothesis differs from lava tube formation in that lava tubes result from constructional, rather than erosional, processes. However, similar to lava tubes, subsurface conduits associated with the stoping hypothesis may provide a more thermally efficient means of transporting lava than a crusted surface flow [*Keszthelyi*, 1995; *Sakimoto and Zuber*, 1998; *Harris et al.*, 2005].

[47] **Acknowledgments.** This work was supported by NASA grants NNG04GG36G and NAG5-13432 to Hansen and the University of Minnesota Duluth and by the McKnight Foundation. Many thanks to G. Komatsu and an anonymous reviewer for thoughtful and thorough reviews which greatly enhanced and improved this manuscript. Discussions with, and comments by, R. Bannister, J. Goodge, I. Lopez, J. Mohr, H. Mooers, K. Riker-Coleman, P. Siders, J. Swenson, C. Teyssier, and D. Young were extremely helpful.

References

Addington, E. A. (2001), A stratigraphic study of small volcano clusters on Venus, *Icarus*, *149*, 16–36.

Aubele, J. C. (1996), Akkruva small shield plains: Definition of a significant regional plains unit on Venus, *Proc. Lunar Planet. Sci. Conf. 27th*, 49–50.

Aubele, J., and E. Slyuta (1990), Small domes on Venus, *Earth Moon Planets*, *50/51*, 452–493.

Baker, V. R., G. Komatsu, T. J. Parker, V. C. Gulick, J. S. Kargel, and J. S. Lewis (1992), Channels and valleys on Venus: Preliminary analysis of Magellan data, *J. Geophys. Res.*, *97*(E8), 13,421–13,444.

Baker, V. R., G. Komatsu, V. C. Gulick, and T. J. Parker (1997), Channels and valleys, in *Venus II*, edited by S. W. Bougher, D. M. Hunten, and R. J. Phillips, pp. 757–793, Univ. of Ariz. Press, Tucson.

Basilevsky, A. T., A. A. Pronin, L. B. Ronca, V. P. Kryuchkov, A. L. Sukhanov, and M. S. Markov (1986), Styles of tectonic deformations on Venus: Analysis of Venera 15 and 16 data, *Proc. Lunar Planet. Sci. Conf. 16th*, Part 2, *J. Geophys. Res.*, *91*(suppl.), D399–D411.

Bloom, A. L. (1998), *Geomorphology: A Systematic Analysis of Late Cenozoic Landforms*, 3rd ed., 482 pp., Prentice Hall, Old Tappan, N. J.

Burbank, D., A. Meigs, and N. Brozovic (1996), Interactions of growing folds and coeval depositional systems, *Basin Res.*, *8*, 199–233.

Bussey, D. B. J., S. A. Sorenson, and J. E. Guest (1995), Factors influencing the capability of lava to erode its substrate: Application to Venus, *J. Geophys. Res.*, *100*(E8), 16,941–16,948.

Carr, M. H. (1974), The role of lava erosion in the formation of lunar sinuous rilles and Martian channels, *Icarus*, *22*, 1–23.

Crisp, D., and D. Titov (1997), The thermal balance of the Venus atmosphere, in *Venus II*, edited by S. W. Bougher, D. M. Hunten, and R. J. Phillips, pp. 353–384, Univ. of Ariz. Press, Tucson.

Crumpler, L. S., J. C. Aubele, D. A. Senske, S. T. Keddie, K. P. Magee, and J. W. Head (1997), Volcanoes and centers of volcanism on Venus, in *Venus II*, edited by S. W. Bougher, D. M. Hunten, and R. J. Phillips, pp. 697–756, Univ. of Ariz. Press, Tucson.

Dawson, J. B., H. Pinkerton, G. E. Norton, and D. M. Pyle (1990), Physiochemical properties of alkali carbonatite lavas: Data from the 1988 eruption of Oldoinyo Lengai, Tanzania, *Geology*, *18*, 260–263.

DeShon, H. R., D. A. Young, and V. L. Hansen (2000), Geological evolution of southern Rusalka Planitia, *J. Geophys. Res.*, *105*(E3), 6983–6995.

Donahue, T. M., D. H. Grinspoon, R. E. Heartle, and R. R. Hodges Jr. (1997), Ion/neutral escape of hydrogen and deuterium: Evolution of water, in *Venus II*, edited by S. W. Bougher, D. M. Hunten, and R. J. Phillips, pp. 385–414, Univ. of Ariz. Press, Tucson.

Donahue, T. M., J. H. Hoffman, R. R. Hodges, and A. J. Watson (1982), Venus was wet: A measurement of the ratio of deuterium to hydrogen, *Science*, *216*, 630–633.

Dragoni, M., A. Piombo, and A. Tallarico (1995), A model for the formation of lava tubes by roofing over a channel, *J. Geophys. Res.*, *100*(B5), 8435–8447.

Engelder, T., and P. Geiser (1980), On the use of regional joint sets as trajectories of paleostress fields during development of the Appalachian Plateau, New York, *J. Geophys. Res.*, *85*, 6319–6341.

Fagents, S. A., and R. Greeley (2001), Factors influencing lava-substrate heat transfer and implications for thermomechanical erosion, *Bull. Volcanol.*, *62*, 519–532.

Fegley, B., Jr., G. Klingelhofer, K. Lodders, and T. Widemann (1997), Geochemistry of surface-atmosphere interactions on Venus, in *Venus II*,

edited by S. W. Bougher, D. M. Hunten, and R. J. Phillips, pp. 591–636, Univ. of Ariz. Press, Tucson.
Ford, J. P., and G. H. Pettengill (1992), Venus topography and kilometer-scale slopes, *J. Geophys. Res.*, *97*(E8), 13,103–13,114.
Ford, J. P., J. J. Plaut, C. M. Weitz, T. G. Farr, D. A. Senske, E. R. Stofan, G. Michaels, and T. J. Parker (1993), Guide to Magellan image interpretation, *Jet Propul. Lab. Publ. 93*, *24*, 148 pp.
Golombek, M. P., J. B. Plescia, B. J. Franklin (1991), Faulting and folding in the formation of planetary wrinkle ridges, *Proc. Lunar Planet. Sci. Conf. 21st*, 679–693.
Greeley, R. (1971), Observations of actively forming lava tubes and associated structures, Hawaii, *Mod. Geol.*, *2*, 207–223.
Greeley, R., S. A. Fagents, R. S. Harris, S. D. Kadel, D. A. Williams, and J. E. Guest (1998), Erosion by flowing lava: Field evidence, *J. Geophys. Res.*, *103*(B11), 27,325–27,345.
Gregg, T. K. P., and R. Greeley (1993), Formation of venusian canali: Consideration of lava types and their thermal behaviors, *J. Geophys. Res.*, *98*(E6), 10,873–10,882.
Guest, J. E., M. H. Bulmer, J. Aubele, K. Beratan, R. Greeley, J. W. Head, G. Michaels, C. Weitz, and C. Wiles (1992), Small volcanic edifices and volcanism in the plains of Venus, *J. Geophys. Res.*, *97*(E8), 15,949–15,966.
Gulick, V. C., G. Komatsu, V. R. Baker, R. G. Strom, and T. J. Parker (1991), Channelson Venus: Preliminary morphological assessment and classification, *Proc. Lunar Planet. Sci. Conf. 22nd*, 507–508.
Hansen, V. L. (2000), Geologic mapping of tectonic planets, *Earth Planet. Sci. Lett.*, *176*, 527–542.
Hansen, V. L. (2005), Venus's shield terrain, *Geol. Soc. Am. Bull.*, *117*, 808–822.
Hansen, V. L., and J. J. Willis (1996), Structural analysis of a sampling of tesserae: Implications of Venus geodynamics, *Icarus*, *123*, 296–312.
Hansen, V. L., and J. J. Willis (1998), Ribbon terrain formation, southwestern Fortuna Tessera, Venus: Implications for lithosphere evolution, *Icarus*, *132*, 321–343.
Harris, A., J. Bailey, S. Calavari, and J. Dehn (2005), Heat loss measured at a lava channel and its implications for down-channel cooling and rheology, in *Kinematics and Dynamics of Lava Flows*, edited by M. Manga and G. Ventura, *Spec. Pap. Geol. Soc. Am.*, *396*, 125–146.
Head, J. W., L. S. Crumpler, J. C. Aubele, J. E. Guest, and R. S. Saunders (1992), Venus volcanism: Classification of volcanic features and structures, associations, and global distribution from Magellan data, *J. Geophys. Res.*, *97*(E8), 13,153–13,197.
Hon, K., J. Denlinger, and K. MacKay (1994), Emplacement and inflation of pahoehoe sheet flows: Observations and measurements of active lava flows on Kilauea Volcano, *Geol. Soc. Am. Bull.*, *106*, 361–370.
Hulme, G. (1973), Turbulent lava flow and the formation of lunar sinuous rilles, *Mod. Geol.*, *4*, 107–117.
Hulme, G. (1974), The interpretation of lava flow morphology, *Geophys. J. R. Astron. Soc.*, *39*, 361–383.
Hulme, G. (1982), A review of lava flow processes related to the formation of lunar sinuous rilles, *Geophys. Surv.*, *5*, 245–279.
Jones, A. P., and K. T. Pickering (2003), Evidence for aqueous fluid-sediment transport and erosional processes on Venus, *J. Geol. Soc. London*, *160*, 319–327.
Jones, J. A. A. (1990), Piping effects in humid lands, in *Groundwater geomorphology; The Role of Subsurface Water in Earth-Surface Processes and Landforms*, edited by C. G. Higgins, and D. R. Coates, *Spec. Pap. Geol. Soc. Am.*, *252*, 111–138.
Kargel, J. S., B. Fegley, A. Treiman, and R. L. Kirk (1994), Carbonatite-sulfate volcanism on Venus, *Icarus*, *112*, 219–252.
Kauahikaua, J., D. R. Sherrod, K. V. Cashman, C. Heliker, K. Hon, T. N. Mattox, and J. A. Johnson (2003), Hawaiian lava-flow dynamics during the Pu'u 'O'o-Kupaianaha Eruption: A tale of two decades, in *The Pu'u 'O'o-Kupainanaha Eruption of Kilauea Volcano, Hawai'i: The First 20 Years*, edited by C. Heliker, D. A. Swanson, and T. J. Takahashi, *U.S. Geol. Surv. Prof. Pap.*, *1676*, 63–88.
Kaula, W. M., A. Lenardic, D. L. Binschadler, and J. Arkani-Hamed (1997), Ishtar Terra, in *Venus II*, edited by S. W. Bougher, D. M. Hunten, and R. J. Phillips, pp. 879–900, Univ. of Ariz. Press, Tucson.
Kerr, R. C. (2001), Thermal erosion by laminar lava flows, *J. Geophys. Res.*, *106*(B11), 26,453–26,465.
Keszthelyi, L. (1995), A preliminary thermal budget for lava tubes on Earth and planets, *J. Geophys. Res.*, *100*(B10), 20,411–20,420.
Kirk, R. L., L. A. Soderblom, and E. M. Lee (1992), Enhanced visualization for interpretation of Magellan radar data–Supplement to the Magellan special issue, *J. Geophys. Res.*, *97*(E8), 16,371–16,380.
Komatsu, G., and V. R. Baker (1994), Meander properties of venusian channels, *Geology*, *22*, 67–70.
Komatsu, G., J. S. Kargel, and V. R. Baker (1992), Canali-type channels on Venus: Some genetic constraints, *Geophys. Res. Lett.*, *19*, 1415–1418.
Komatsu, G., V. R. Baker, V. C. Gulick, and T. J. Parker (1993), Venusian channels and valleys: Distribution and volcanological implications, *Icarus*, *102*, 1–25.
Komatsu, G., V. C. Gulick, and V. R. Baker (2001), Valley networks on Venus, *Geomorphology*, *37*, 225–240.
Lutter, W. J., R. D. Catchings, and C. M. Jarchow (1994), An image of the Columbia Plateau from inversion of high-resolution seismic data, *Geophysics*, *59*, 1278–1289.
Marquez, A., M. A. de Pablo, R. Oyarzun, and C. Viedma (2005), Evidence of gully formation by regional groundwater flow in the Gorgoum-Newton region (Mars), *Icarus*, *179*, 398–414.
McGill, G. E. (1993), Wrinkle ridges, stress domains, and kinematics of venusian plains, *Geophys. Res. Lett.*, *20*, 2407–2410.
Mege, D., and R. E. Ernst (2001), Contractional effects of mantle plumes on Earth, Mars, and Venus, in *Mantle Plumes: Their Identification Through Time*, edited by R. E. Ernst and K. L. Buchan, *Spec. Pap. Geol. Soc. Am.*, *352*, 103–140.
Oshigami, S., and N. Namiki (2005), Cross-sectional profile of Baltis Vallis channel on Venus: Reconstruction from Magellan SAR brightness data, *Proc. Lunar Planet. Sci. Conf. 36th*, Abstract 1555.
Parker, Sr., G. G., C. G. Higgins, and W. W. Wood (1990), Piping and pseudokarst in drylands, with case studies by G. G. Parker Sr. and W. W. Wood, in *Groundwater Geomorphology; The Role of Subsurface Water in Earth-Surface Processes and Landforms*, edited by C. G. Higgins and D. R. Coates, *Spec. Pap. Geol. Soc. Am.*, *252*, 77–110.
Pederson, D. T. (2001), Stream piracy revisited: A groundwater-sapping solution, *GSA Today*, *11*, 4–10.
Plescia, J. B., and M. P. Golombek (1986), Origin of planetary wrinkle ridges based on the study of terrestrial analogs, *Geol. Soc. Am. Bull.*, *97*, 1289–1299.
Pollard, D. D., and A. Aydin (1988), Progress in understanding jointing over the past century, *Geol. Soc. Am. Bull.*, *100*, 1181–1204.
Price, N., and J. Cosgrove (1990), *Analysis of Geological Structures*, 502 pp., Cambridge Univ. Press, New York.
Reidel, S. P., R. K. Ledgerwood, C. W. Myers, M. G. Jones, and R. D. Landon (1980), Rate of deformation in the Pasco Basin during the Miocene as determined by distribution of Columbia River Basalt flows, *Geol. Soc. Am. Abstr. Programs*, *12*(3), 149.
Sakimoto, S. E. H., and M.T. Zuber (1998), Flow and convective cooling in lava tubes, *J. Geophys. Res.*, *103*(B11), 27,465–27,487.
Skinner, J. A., and K. L. Tanaka (2003), How should planetary map units be defined?, *Proc. Lunar Planet. Sci. Conf. 34th*, Abstract 2100.
Snyder, D. (2002), Cooling of lava flows on Venus: The coupling of radiative and convective heat transfer, *J. Geophys. Res.*, *107*(E10), 5080, doi:10.1029/2001JE001501.
Stofan, E. R., A. W. Brian, and J. E. Guest (2005), Resurfacing styles and rates on Venus: Assessment of 18 venusian quadrangles, *Icarus*, *173*, 312–321.
Tanaka, K. L., et al. (1994), The Venus Geologic Mapper's Handbook, 2nd ed., *U.S. Geol. Surv. Open File Rep.*, *94–438*, 68 pp.
Watters, T. R. (1988), Wrinkle ridge assemblages on the terrestrial planets, *J. Geophys. Res.*, *93*, 10,236–10,254.
Watters, T. R. (1991), Origin of periodically spaced wrinkle ridges on the Tharsis Plateau of Mars, *J. Geophys. Res.*, *96*, 15,599–15,616.
Wilhelms, D. E. (1990), Geologic mapping, in *Planetary Mapping*, edited by R. Greeley, and R. M. Batson, pp. 208–260, Cambridge Univ. Press, New York.
Williams, D. A., R. C. Kerr, and C. M. Lesher (1998), Emplacement and erosion by Archaen komatiite lava flows at Kambalda: Revisited, *J. Geophys. Res.*, *103*(B11), 27,533–27,550.
Williams, D. A., S. D. Kadel, R. Greeley, C. M. Leshner, and M. A. Clynne (2004), Erosion by flowing lava: Geochemical evidence in the Cave Basalt, Mt. St. Helens, Washington, *Bull. Volcanol.*, *66*, 168–181.
Williams-Jones, G., A. E. Williams-Jones, and J. Stix (1998), The nature and origin of venusian canali, *J. Geophys. Res.*, *103*, 8545–8555.
Winter, J. D. (2001), An introduction to igneous and metamorphic petrology, 697 pp., Prentice Hall, Old Tappan, N. J.
Wohl, E. E., and H. Achyuthan (2002), Substrate influence on incised-channel morphology, *J. Geol.*, *110*, 115–120.
Young, D. A., and V. L. Hansen (2003), Geologic map of the Rusalka Planitia Quadrangle (V-25), Venus, *U.S. Geol. Surv. Misc. Geol. Invest. Ser.*, *I-2783*, 1:5,000,000 scale.
Zimbelman, J. R. (2001), Image resolution and evaluation of genetic hypotheses for planetary landscapes, *Geomorphology*, *37*, 179–199.

V. L. Hansen and N. P. Lang, Department of Geological Sciences, University of Minnesota Duluth, Duluth, MN 55812, USA. (lang0604@tc.umn.edu)